Available online at www.sciencedirect.com

SciVerse ScienceDirect

Procedia Computer Science 18 (2013) 2117 – 2126

Procedia
Computer Science

2013 International Conference on Computational Science

The Discretization Method for Convention-Diffusion Equations in Two-Dimensional Cylindrical Coordinate Systems Based on Unstructured Grids

Guojun Yu, Bo Yu*, Yu Zhao, Qianqian Shao, Jianyu Xie

National Engineering Laboratory for Pipeline Safety, Beijing Key Laboratory of Urban Oil and Gas Distribution Technology, China University of Petroleum (Beijing), Beijing 102249, PR China

Abstract

The study on the application of unstructured grids in solving two-dimensional cylindrical coordinates (*r-z*) problems is scarce, since one of the challenges is the accurate calculation of the control volumes. In this paper, an unstructured grids-based discretization method, in the framework of a finite volume approach, is proposed for the solution of the convection-diffusion equation in an *r-z* coordinate. Numerical simulations are presented for the natural convection problem. The numerical results of the proposed method are found to be accurate. The employment of unstructured grids leads to flexibility of the discretization method for irregular domains of any shapes.

Keywords: Cylindrical coordinate; Unstructured grid; Control volume; Discretization method; Finite volume method

1. Introduction

Cylindrical symmetrical problems are usually involved in the calculations of heat transfer and fluid flow. In many cases, due to the symmetry of the computation domain and the solution of the physical problem, the numerical solution of the flow equations could be greatly simplified by expressing both the governing equations and the initial/boundary conditions in a two-dimensional cylindrical coordinate system. Actually, many practical problems could be simplified from three-dimensional ones to two-dimensional ones (*r-z* or $r\text{-}\theta$).

* Corresponding author. Tel.: +86-10-8973-3849; fax: +86-10-8973-3849.
E-mail address: yubobox@vip.163.com.

doi:10.1016/j.procs.2013.05.382

Nomenclature

a	an arbitrary vector	μ	dynamic viscosity
A	bounding surface of a control volume	ν	kinematic viscosity
d	direction vector	ρ	density
F_j	mass flux at surface j	ϕ	general variable
Gr	Grashof number	*Subscripts:*	
n	unit vector normal to the surface element	c	cool
p	pressure	CV	control volume
Pr	Prandtl number	h	high
r	radius vector	i	node number
r, θ, z	radial , angular and axial coordinate respectively	j	face number of a control volume
S	general source term	P_0	interested node number
T	temperature	*Superscripts:*	
u, v	radial and axial velocity component respectively	*	representing dimensionless
Greek Symbols:		*Prefixes:*	
α	thermal diffusivity	Δ	increment
β	coefficient of thermal expansion	∇	gradient
Γ	general diffusion coefficient		

Some previous applications of the two-dimensional cylindrical coordinates to the solution of the three-dimensional cylindrical symmetrical problems are listed below. Bilgili and Ataer [1] investigated the heat and mass transfer for hydrogen absorption in an annular metal hydride bed by a two-dimensional cylindrical coordinate system. Oliveski et al. [2] analyzed the velocity and temperature fields inside a tank submitted to internal natural and mixed convection using a two-dimensional model in the cylindrical coordinate system through the finite volume method. Yang and Tsai [3] presented a numerical study of transient conjugate heat transfer in a high turbulence air jet impinging over a flat circular disk using a finite volume method in the two-dimensional cylindrical coordinate system. Oliveski et al. [4] investigated the thermal stratification inside a tank containing thermal oil by a two-dimensional model in the cylindrical coordinate system with the finite volumes method. Sievers et al. [5] employed a two-dimensional anisotropic cylindrical coordinate model with linear triangular finite elements to simulate the steady-state temperature distribution within the Li-ion cells.

The computational domains in previous reports [1-6] are all regular ones, and are all discretized by orthogonal grids. A few reports [7] presented the employment of unstructured grids in two-dimensional cylindrical problems, but their concern was the physical problem in $r-\theta$ plane (actually a polar coordinate system), neglecting the gradient in z direction, and thus is different from the issue we concern in the $r-z$ plane. To the author's knowledge, the study on the applications of unstructured grids in the solution of convection-diffusion problems in two-dimensional $r-z$ coordinates is not found, and the discretization method especially the calculation of the control volume has not been reported.

A regular $r-z$ cylindrical symmetrical domain could be mapped by completely orthogonal grids; while an irregular $r-z$ domain could not be mapped by orthogonal grids directly, but could be perfectly mapped by unstructured grids. If the unstructured grids are applied in a two-dimensional cylindrical coordinate system ($r-z$), one challenge is the accurate calculation of the control volume. For structured grids, the calculation of the control volume is easy, i.e. $V_i = 0.5 r_{P_0} \Delta r_{P_0} \Delta z_{P_0}$, since Δr_{P_0} and z_{P_0} are available on a given mesh. But for the unstructured grids in a two-dimensional cylindrical coordinate system, as the grid face is not parallel to the coordinate axes, plus different grid cells are of different shapes and sizes, the calculation of such control volumes is complicated.

In this article, an unstructured grids-based discretization method, in the framework of a finite volume approach, is proposed for the solution of the convection-diffusion equations in $r-z$ coordinates, and especially an accurate calculation method of the control volumes is presented. After that, the discretization method is validated by a well-designed numerical case.

2. Governing equations and discretization method

In the two-dimensional cylindrical coordinate, continuity equation, momentum equation and energy equation of steady state can be described by a general governing equation:

$$\frac{\partial}{\partial z}\left(\rho u \phi\right) + \frac{1}{r}\frac{\partial}{\partial r}\left(r \rho v \phi\right) = \frac{\partial}{\partial z}\left(\Gamma \frac{\partial \phi}{\partial z}\right) + \frac{1}{r}\frac{\partial}{\partial r}\left(r \Gamma \frac{\partial \phi}{\partial r}\right) + S \tag{1}$$

The two terms on the left hand side of the equation are the convection terms; the first two terms on the right hand side are the diffusion terms, and the last term is the general source term.

Define $r^* = \frac{r}{L}$, $z^* = \frac{z}{L}$, $u^* = \frac{\rho L}{\mu} u$, $v^* = \frac{\rho L}{\mu} v$, $T^* = \frac{T - T_c}{T_h - T_c}$, $p^* = \frac{\rho L^2}{\mu^2} p + \frac{\rho^2 g L^2}{\mu^2} z$, $\mathrm{Gr} = \frac{\rho^2 \beta g \left(T_h - T_c\right) L^3}{\mu^2}$, and the dimensionless type of Eq. (1) is derived

$$div(\mathbf{U}^* \phi^*) - div(\Gamma^* grad \phi^*) = S^* \tag{2}$$

where $\mathbf{U}$ represents the velocity vector, $\mathbf{U} = ui + vj$.

The details of Eq. (1) and Eq. (2) for a natural convection problem are listed in Table 1. In this table, the underlined part is the buoyancy lift which is treated by a Boussinesq assumption.

2.1 An unstructured grids-based finite volume discretization method

On unstructured grids, the steady-state dimensionless convection-diffusion equation in a tensor form is given by Eq. (2).

Integrating Eq. (2) over the control volume CV gives:

$$\int_{CV} div(\mathbf{U}^* \phi^*) dV^* - \int_{CV} div(\Gamma^* grad \phi^*) dV^* = \int_{CV} S^* dV^* \tag{3}$$

Table 1. Coefficients and source terms of both dimensional and dimensionless governing equations for natural convection problems

Equation type		ϕ	Γ	S	ϕ^*	Γ^*	S^*
Continuity equation		1	0	0	1	0	0
Momentum equation		u	μ	$-\frac{\partial p}{\partial r}-\frac{\mu u}{r^2}$	u^*	1	$-\frac{\partial p^*}{\partial r^*}-\frac{u^*}{r^{*2}}$
		v	μ	$-\frac{\partial p}{\partial z}+\underline{\rho g\beta(T-T_c)}$	v^*	1	$-\frac{\partial p^*}{\partial z^*}+\underline{\mathrm{Gr}\,T^*}$
Energy equation		T	$\frac{\mu}{\Pr}$	0	T^*	$\frac{1}{\Pr}$	0

Application of Gauss theorem to Eq. (3) gives

$$\int_A \mathbf{n}\cdot(\mathbf{U}^*\phi^*)dA^* - \int_A \mathbf{n}\cdot(\Gamma^* grad\phi^*)dA^* = \int_{CV} S^*_{P_0} dV^* \tag{4}$$

The area integrations are carried out over all surface segments, so Eq. (4) can be written as follows:

$$\sum_{all\,surfaces}\int_{\Delta A_j}\mathbf{n}_j\cdot(\mathbf{U}^*\phi^*)dA^* - \sum_{all\,surfaces}\int_{\Delta A_j}\mathbf{n}_j\cdot(\Gamma^* grad\phi^*)dA^* = \int_{CV} S^*_{P_0} dV^* \tag{5}$$

The first term on the left hand side is discretized as follows:

$$\sum_{all\,surfaces}\int_{\Delta A_j}\mathbf{n}_j\cdot(\mathbf{U}^*\phi^*)dA^* = \sum_{all\,surfaces} F_j\phi^*_j \tag{6}$$

And the second term on the left hand side is discretized as follows:

$$D_j = -\int_{\Delta A_i}\mathbf{n}_j\cdot(\Gamma^* grad\phi^*)dA^* = -\mathbf{n}_j\cdot(\Gamma^* grad\phi^*)\Delta A^*_j \tag{7}$$

D_j, the diffusion term, is divided into two components, a normal component and a cross-diffusion component:

$$D_j = D^n_j + D^c_j \tag{8}$$

$$D^n_j = \mathbf{n}_j\cdot\left(\frac{\phi^*_{P_j}-\phi^*_{P_0}}{\left|\mathbf{d}^*_j\right|}\frac{\mathbf{d}^*_j}{\left|\mathbf{d}^*_j\right|}\right)\Gamma^*_j\Delta A^*_j \tag{9}$$

$$D_j^c = \mathbf{n}_j \cdot \left(\nabla\phi_j^* - \nabla\phi_j^* \cdot \frac{\mathbf{d}_j^*}{\left|\mathbf{d}_j^*\right|} \cdot \frac{\mathbf{d}_j^*}{\left|\mathbf{d}_j^*\right|} \right) \Gamma_j^* \Delta A_j^* \tag{10}$$

The gradient on the surface j is determined by

$$\nabla\phi_{P_j}^* = \nabla\phi_{P_0}^* \frac{\left|\mathbf{r}_j^* - \mathbf{r}_{P_j}^*\right|}{\left|\mathbf{d}_j^*\right|} + \nabla\phi_{P_j}^* \frac{\left|\mathbf{r}_{P_0}^* - \mathbf{r}_j^*\right|}{\left|\mathbf{d}_j^*\right|} \tag{11}$$

The source term is discretized as

$$\int_{CV} S_{P_0}^* dV = S_{P_0}^* \Delta V_{P_0}^* \tag{12}$$

where $\Delta V_{P_0}^*$ is the control volume of node P_0.

For the unstructured triangular grids, substituting Eqs. (6)—(12) into Eq. (5) gives

$$\sum_{j=1}^{3} F_j \phi_j^* - \sum_{j=1}^{3} \mathbf{n}_j \cdot \left(\frac{\phi_{P_j}^* - \phi_{P_0}^*}{\left|\mathbf{d}_j^*\right|} \frac{\mathbf{d}_j^*}{\left|\mathbf{d}_j^*\right|} \right) \Gamma_j^* \Delta A_j^* - \sum_{j=1}^{3} \mathbf{n}_j \cdot \left(\nabla\phi_j^* - \nabla\phi_j^* \cdot \frac{\mathbf{d}_j^*}{\left|\mathbf{d}_j^*\right|} \cdot \frac{\mathbf{d}_j^*}{\left|\mathbf{d}_j^*\right|} \right) \Gamma_j^* \Delta A_j^* = S_{P_0}^* \Delta V_{P_0}^* \tag{13}$$

In Eq. (13),

$$\phi_j^* = \max\left(F_j, 0\right)\left[\phi_{P_0}^* + \left(\nabla\phi^*\right)_j \cdot \left(\mathbf{r}_j^* - \mathbf{r}_{P_0}^*\right)\right] - \max\left(-F_j, 0\right)\left[\phi_{P_j}^* + \left(\nabla\phi^*\right)_j \cdot \left(\mathbf{r}_j^* - \mathbf{r}_{P_j}^*\right)\right] \tag{14}$$

So, the discretized equation is obtained as follows:

$$a_{P_0} \phi_{P_0}^* = \sum_{j=1}^{3} a_j \phi_j^* + b \tag{15}$$

where

$$b = \sum_{j=1}^{3} \left(\begin{array}{l} -\max\left(F_j, 0\right)\left(\nabla\phi^*\right)_j \cdot \left(\mathbf{r}_j^* - \mathbf{r}_{P_0}^*\right) + \max\left(-F_j, 0\right)\left(\nabla\phi^*\right)_j \cdot \left(\mathbf{r}_j^* - \mathbf{r}_{P_j}^*\right) + \\ \mathbf{n}_j \cdot \left(\nabla\phi_j^* - \nabla\phi_j^* \cdot \frac{\mathbf{d}_j^*}{\left|\mathbf{d}_j^*\right|} \cdot \frac{\mathbf{d}_j^*}{\left|\mathbf{d}_j^*\right|} \right) \Gamma_j^* \Delta A_j^* + S_{P_0}^* \Delta V_{P_0}^* \end{array} \right) + S_{P_0}^* \Delta V_{P_0}^* \tag{16}$$

$$a_j = \mathbf{n}_j \cdot \frac{\mathbf{d}_j^*}{\left|\mathbf{d}_j^*\right|^2} \Gamma_j^* \Delta A_j^* + \left(\max(F_j, 0) - F_j\right) \tag{17}$$

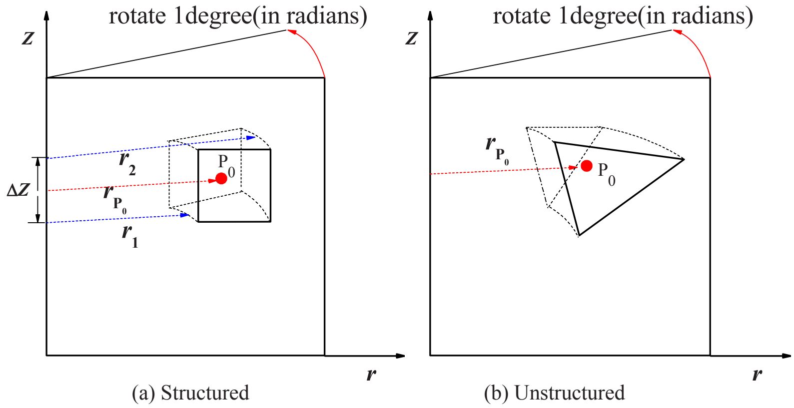

Fig. 1. Sketch map of structured and unstructured control volumes in a two-dimensional cylindrical coordinate system

$$a_{P_0} = \sum_{i=1}^{3} a_j - S^*_{P_0}\phi^*_{P_0} \tag{18}$$

Eqs. (15)—(18) are applicable to any coordinate system with different calculations of surface element area ΔA_j and control volume ΔV_{P_0} . Taking structured mesh as an example, in a two-dimensional Cartesian coordinate system, $\Delta A_j = \Delta r_{P_0}$ (the surface parallel to the *r* axis) or $\Delta A_j = \Delta z_{P_0}$ (the face parallel to the *z* axis) and the control volume can be determined by $\Delta V_{P_0} = \Delta r_{P_0}\Delta z_{P_0}$; while in a two-dimensional cylindrical coordinate system, face vector $\Delta A_j = r_j \Delta z_{P_0}$ (the left and right faces) or $\Delta A_j = r_{P_0}\Delta r_{P_0}$ (the upper and lower faces) and the control volume can be calculated by $\Delta V_{P_0} = 0.5 r_{P_0}\Delta r_{P_0}\Delta z_{P_0}$ (shown in Fig. 1(a)). For unstructured grids in a two-dimensional cylindrical coordinate system, the calculation of each face factor is also easy to perform, i.e. $\Delta A_j = r_j L_j$ (here r_j is the *r* coordinate of the midpoint at *j*th boundary segment, and L_j is the length of the *j*th boundary segment), but the calculation of control volume is complicated since the control volume is an irregular pentahedron as sketched in Fig. 1(b), of which the size and shape are dependent on the relative position of the three vertexes. The calculation of the control volume could not be determined by the same procedures as structured grids' and require complicated procedures which will be proposed in the following section.

2.2 An accurate calculation method of unstructured control volumes in a two-dimensional cylindrical coordinate system

In this section, an accurate calculation method of the unstructured control volume is proposed. It is known that, a solid of revolution formed by rotating a right trapezoid by 360 degrees is a circular truncated cone as shown in Fig. 2, the volume of which is easy to calculate by

$$V = \frac{\pi}{3} H\left(R^2 + r^2 + Rr\right) \tag{19}$$

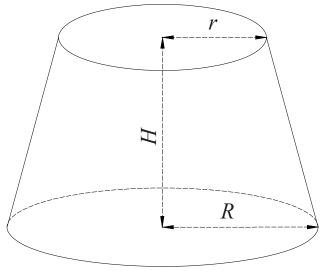

Fig. 2 Circular truncated cone formed by rotating a right trapezoid by 360 degrees

A right trapezoid can be constructed by each edge of the triangular cell, two lines parallel to *r*-axis, plus *z*-axis. The right trapezoids involving edges *AB*, *BC* and *AC* are named *A1*, *A2* and *A3* respectively, and examples could be found in Fig. 3(a) and Fig. 3(b) . Since the area of the triangular cell is the algebraic sum of *A1*, *A2* and *A3*, the solid of revolution by rotating the triangle *ABC* about *z*-axis by 360 degrees could be determined by the combination of three circular truncated cones formed by rotating *A1*, *A2* and *A3*.

Define vertex *A* is the one with the smallest *r*, *B* is the one with the greater *z* between the others two points and *C* is the remaining one. The coordinates of *A*, *B* and *C* are respectively (r_1, z_1), (r_2, z_2) and (r_3, z_3). Due to the different relative positions of the three vertexes of a triangular cell, algebraic sum of *A1*, *A2* and *A3* may be different.

Based on the above assumptions, there are 6 different relative positions of the three vertexes of a triangle, i.e. ($z_1 < z_3 < z_2$ and $r_2 < r_3$), ($z_1 < z_3 < z_2$ and $r_2 > r_3$), ($z_3 < z_2 < z_1$ and $r_2 < r_3$), ($z_3 < z_2 < z_1$ and $r_2 > r_3$), ($z_3 < z_1 < z_2$ and $r_2 < r_3$) and ($z_3 < z_1 < z_2$ and $r_2 > r_3$). If $z_1 < z_3 < z_2$ or $z_3 < z_2 < z_1$, the area of triangular *ABC* is $S_{\Delta ABC} = A_1 + A_2 - A_3$ regardless of *r*. If $z_3 < z_1 < z_2$ the area of triangular *ABC* is $S_{\Delta ABC} = A_2 - A_1 - A_3$ regardless of *r*. So, there are only two situations in total, i.e. $z_1 < z_3 < z_2$ or $z_3 < z_2 < z_1$ (situation 1, Fig. 3(a)), and $z_3 < z_1 < z_2$ (situation 2, Fig. 3(b)).

For situation 1, taking $r_2 > r_3$ as an example, the combination and split method to determine the control volume is shown in Fig. 3(a). The stereogram of the triangular control volume is shown in Fig. 4(a).

Since $S_{\Delta ABC} = A_1 + A_3 - A_2$ and V_1, V_2 and V_3 can be calculated by Eq. (18), we have,

$$V_{ABC} = V_1 + V_2 - V_3 = \frac{\pi}{3} \times \left[(z_1 - z_2)(r_1^2 + r_2^2 + r_1 r_2) + (z_2 - z_3)(r_2^2 + r_3^2 + r_2 r_3) - (z_1 - z_3)(r_1^2 + r_3^2 + r_1 r_3) \right]$$

The control volume of triangle *ABC* (rotated by 1degree as shown in Fig. 3(a)) is,

$$V_{CV} = \frac{V_{ABC}}{2\pi} = \frac{1}{6} \times \left[(z_1 - z_2)(r_1^2 + r_2^2 + r_1 r_2) + (z_2 - z_3)(r_2^2 + r_3^2 + r_2 r_3) - (z_1 - z_3)(r_1^2 + r_3^2 + r_1 r_3) \right]$$

For situation 2, taking $r_2 < r_3$ for example, the combination and split method is shown in Fig. 3(b). The stereogram of the triangular control volume is shown in Fig. 4(b).

Similarly with situation 1, we have,

$$V_{CV} = \frac{V_{ABC}}{2\pi} = \frac{1}{6} \times \left[(z_2 - z_3)(r_2^2 + r_3^2 + r_2 r_3) - (z_2 - z_1)(r_1^2 + r_2^2 + r_1 r_2) - (z_1 - z_3)(r_1^2 + r_3^2 + r_1 r_3) \right]$$

The unstructured control volume could be determined conveniently by the above mentioned combination and split methods. Although the method is performed on the triangular grids, same procedures could be straightforwardly extended to that on an unstructured quadrilateral grids system.

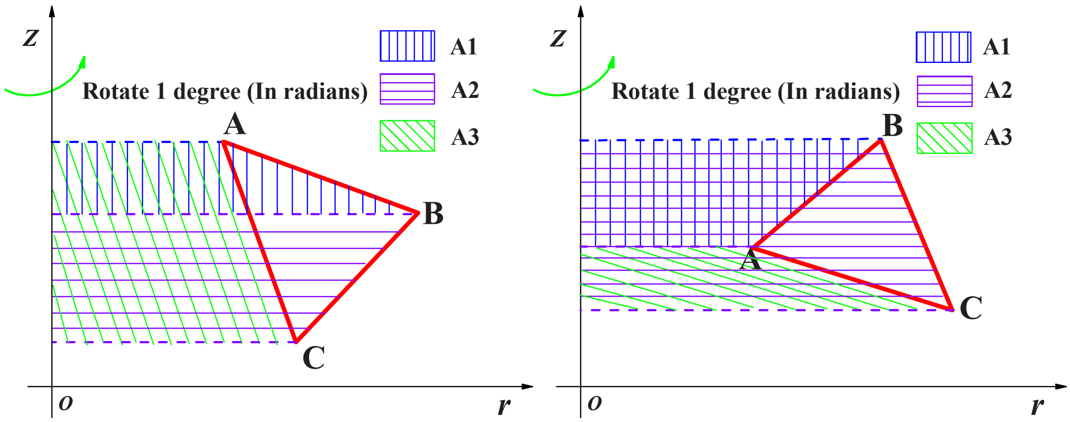

(a) situation1 (b) situation 2

Fig. 3. Combination and split method to determine the control volume

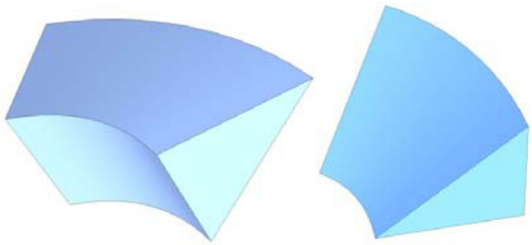

(a) situation 1 (b) situation 2

Fig. 4. The stereogram of the triangular control volume

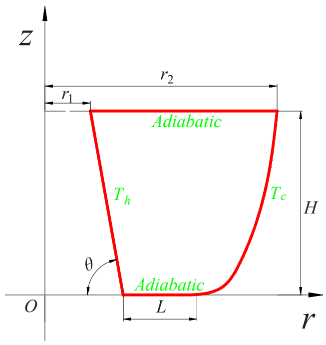

Fig. 5. Computational domain and boundary conditions

3. Numerical examples and results discussions

An example is well devised for an irregular domain to verify the correctness of the proposed unstructured grids-based discretization method. In this Example, the natural convection in an irregular cylindrical cavity is investigated. The three-dimensional cavity is a solid of revolution formed by rotating the geometry shape shown in Fig. 5 about z-axis by 360 degrees. In the figure, the length of the upper boundary is r_2-r_1=H=1m, the height H=1m, and the length of the lower boundary L=0.4m. The right curve boundary is determined by a cubic curve defined as $z=\frac{1+r_1}{0.4^3}\left[r-(r_1+0.6)\right]^3$. The left and right boundaries are of the first-type boundary conditions, with higher temperature of T_h at the left boundary and cooler temperature of T_c on the right one and insulated boundary condition for the upper and lower boundaries.

Figure 6 presents the structured and unstructured grid systems (a coarse one) for the irregular domain. For the irregular domain shown in Fig. 5, it is impossible to map it with orthogonal structured grids, but it can be mapped perfectly by the unstructured grids such as triangular grids Fig. 6(b).

To validate the proposed method, the irregular domain is involved in a square domain shown in Fig. 6(a), and this square domain could be mapped by orthogonal structured grids. Under this circumstance, the boundary

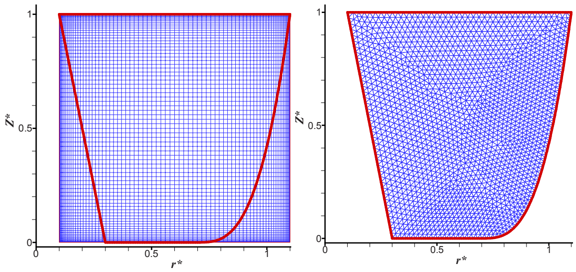

(a) structured (b) unstructured

Fig. 6. The grid system in the selected case

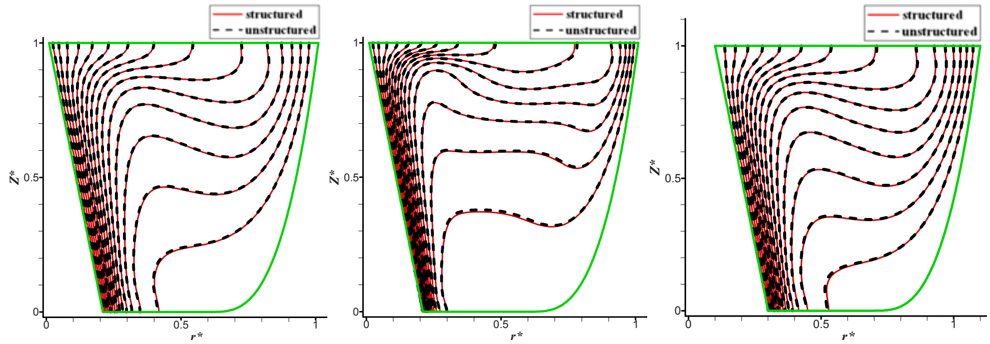

(a) $r_1^* = 0.01$, $\mathrm{Gr} = 10^5$ (b) $r_1^* = 0.01$, $\mathrm{Gr} = 10^6$ (c) $r_1^* = 0.1$, $\mathrm{Gr} = 10^5$

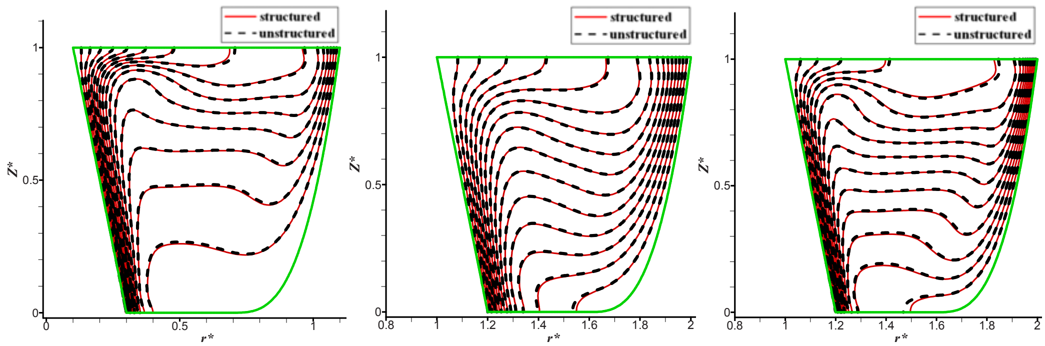

(d) $r_1^* = 0.1$, $\mathrm{Gr} = 10^6$ (e) $r_1^* = 1.00$, $\mathrm{Gr} = 10^5$ (f) $r_1^* = 1.00$, $\mathrm{Gr} = 10^6$

Fig. 7. Comparison of temperature fields with different computation parameters

conditions are affected on the nodes which are adjacent to the real boundary. If the grids are dense enough, this method is acceptable. With the computation parameters as shown in Table 2, a group of results are calculated on the structured grid system with dense enough cells, and chosen to be reference solutions. The results calculated by the unstructured grids are compared with these reference solutions, as shown in Fig. 7. In Table 2, $r_1^* = r_1/(r_1+H)$, $r_1^* = r_2/(r_2+H)$.

It can be seen that the results of the two methods agree well with each other. With structured grids, large amount of grid cells are required to approximate the irregular domain and the treatment of the boundary condition is complicated, while the unstructured grids present very good flexibility to the irregular domain and thus lead to more accurate results than that of structured grids for an irregular domain.

Table 2. Computation parameters in the selected case

Case number	r_1^*	r_1^* / r_2^*	Gr
1	0.01	0.0099	10^5
2	0.01	0.0099	10^6
3	0.1	0.0909	10^5
4	0.1	0.0909	10^6
5	1.0	0.5	10^5
6	1.0	0.5	10^6

The numerical example demonstrated above indicates that the proposed unstructured grids-based discretization method for the convection-diffusion equations is reasonable and accurate.

4. Conclusions

This article proposes an unstructured grids-based discretization method for the convection-diffusion equations in *r-z* coordinate, in the framework of a finite volume approach. Numerical results have validated the correctness of the proposed method. Although, the proposed discretization method is performed only on unstructured triangular grids, it could be readily extended to that on an unstructured quadrilateral grids system. The study provides great convenience for the application of unstructured grids in a two-dimensional cylindrical coordinate system, leading to the flexibility of the discretization method for the irregular domains of any shapes.

Acknowledgements

The study is supported by National Science Foundation of China (Nos. 51134006， 51176204 and 51276198).

References

[1] Bilgili M, Ataer ÖE. Numerical analysis of hydrogen absorption in a P/M metal bed. *Powder Technol.* 2005;**160**:141 – 148.
[2] Oliveski RDC, Krenzinger A, Vielmo HA. Comparison between models for the simulation of hot water storage tanks. *Sol. Energy* 2003; **75**: 121–134.
[3] Yang YT, Tsai SY. Numerical study of transient conjugate heat transfer of a turbulent impinging jet. *Int. J. Heat Mass Tran.*2007;**50**: 799–807.
[4] Oliveski RDC, Macagnan MH, Copetti JB, Petroll ADLM. Natural convection in a tank of oil: experimental validation of a numerical code with prescribed boundary condition. *Exp. Therm. Fluid Sci.*2005;**29**:671–680.
[5] Sievers M, Sievers U, Mao SS. Thermal modelling of new Li-ion cell design modifications. *Forsch. Ingenieurwes.*2010;**74**:215–231.
[6] Li W, Yu B, Wang X, Wang P, Sun S. A finite volume method for cylindrical heat conduction problems based on local analytical solution. *Int. J. Heat Mass Tran.*2012;**55**:5570–5582.
[7] Oosterlee CW, Wesseling P, Segal A. Benchmark solutions for the incompressible Navier-Stokes equations in general coordinates on staggered grids. *Int. J. Numer. Meth. Fl.*1993;**17**:301-321.